Focused Sound Sources and the Acoustical Society of New Zealand Logo

M. A. Poletti

Callaghan Innovation, PO Box 31-310, Lower Hutt

An original refereed contribution to New Zealand Acoustics

Abstract

This paper demonstrates that the logo of the New Zealand Acoustical Society has a sound physical basis. The logo shows concentric circles with a discontinuity between the right and left hemispheres. If the logo were a sound field, these discontinuities would represent amplitude inversions. This behaviour occurs in sound fields containing focused sources, where circular wavefronts converge on a focal point from one hemisphere and then diverge into the other hemisphere. At certain times during the propagation of the wavefronts, the quadrature part of the sound field is maximum, and this demonstrates concentric wavefronts with a phase discontinuity between the two hemispheres and a null along the line separating the two.

Introduction

The logo of the Acoustical Society of New Zealand is a set of grey concentric rings, with the rings in one half-space positioned at radii between the radii of the rings in the other half-space. The logo can be seen on the cover of the journal (with an additional emphasis to show which quarter it has appeared in) and on the website of the society (www.acoustics.org.nz). In keeping with aim of the society to "promote the science and practice of acoustics" (www.acoustics.org.nz/files/ASNZ_Rules.pdf), it is incumbent upon us to ask whether the Society's logo represents a physical sound field. This article demonstrates that this is the case, and that our logo has a sound scientific basis. A sound field that looks very similar to the logo is produced by a focused source, in which circular wavefronts converge to a point and then radiate outwards from that point. This article gives a description of how focused sources are produced and provides methods for generating them.

Focusing of sound is a well-known high-frequency phenomenon in which sound rays converge to a point in space and then diverge from that point. Focusing can occur, for example, when a plane wave is reflected from a curved surface [1][2]. At low frequencies where the wavelength of the plane wave is of similar size to, or larger than, the reflecting object sound tends to dif-fract around the reflector and focusing does not occur. At high frequencies where the wavelength is small compared to the reflecting object, geometric acoustics applies and the behaviour is equivalent to the optical case. In this case, a plane wave parallel to the principal axis of a spherically curved surface will reflect sound to the focal point of the surface. The reflected sound converges on the focal point and then diverges out-wards from the focal point with spherical wave fronts.

Focusing can also be produced by a planar surface if the surface is vibrating in a particular manner. This fact is the basis for the generation of focused sources in sound reproduction systems. For example, Wave field Synthesis (WFS) is a method of producing sound fields derived from the Kirchhoff Helmholtz integral, for an arbitrarily shaped volume of space, or in the simpler case of a planar surface, the Rayleigh integrals [3]–[6]. A large 2D planar array of loudspeakers allows a practical implementation of the first Rayleigh integral and can generate a sound field in front of the array produced by an arbitrary distribution of sources behind the array. Since the array is planar, it also generates the same sound field behind the array. If the sound produced by the array elements are reversed in time, the array produces a sound field that propagates back from the array to the original sound sources. This techniques, known as time reversal signal processing, is used in many areas in optics, ultrasonic imaging [7] and acoustics [8][9]. Focused sources may also be generated in WFS to produce the impression of sound originating in front of the array [10]–[12].

In this paper, we will present the theory of sound field reproduction based on the use of integral formulas. We will then consider the special case of time reversal processing and show how it produces focused sources. We will consider a single sound source for simplicity. We will then consider methods for directly generating focused sound sources. For simplicity we will primarily consider the 2D case, but will include a derivation of a focused source in the 3D case. We also make the standard assumption that sound sources have a complex time dependence of the form $exp(i\omega t)$ where f is the frequency of oscillation and $\omega = 2\pi f$ is the radian frequency. Solutions to the wave equation are then complex functions of space which we denote $q(x,y,z)$. The physical sound pressure p(x,y,z,t) is then the real part of the complex time-varying sound pressure, i.e. Eqn(1):

$$\begin{aligned} p(x,y,z,t) &= \mathrm{Re}\left\{ q(x,y,z)\, e^{i\omega t} \right\} \\ &= q_R(x,y,z)\cos(\omega t) \\ &\quad - q_I(x,y,z)\sin(\omega t) \end{aligned} \tag{1}$$

where $q_R(x,y,z)$ is the real or in-phase part of the complex pressure and $q_I(x,y,z)$ is the imaginary or quadrature part. e see that the physical field contains both in-phase and quadrature components.

INTEGRAL FORMULAS FOR CALCULATION OF SOUND PRESSURE

The reproduction of sound fields is based on integral formulas that allow the calculation of the sound pressure at a point in space given knowledge of the pressure or velocity (or both) on a defined surface. The Kirchhoff–Helmholtz (K–H) integral describes the sound pressure inside a region of space, in which there are no sound sources, as an integral over the surface, S, of the pressure, and the normal component of the pressure gradient, produced on the surface by sound sources outside the region [13] (Fig. 1).

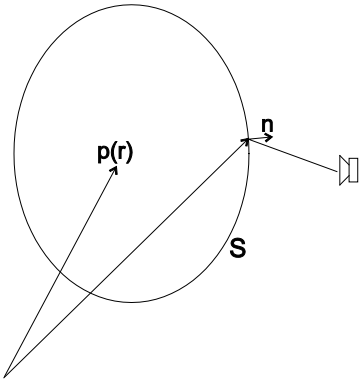

Figure 1: Kirchhoff Helmholtz integral.

Mathematically the integral is expressed, for vectors **r** and **r'**

$$q(\mathbf{r}) = \iint \left[G(\mathbf{r} \mid \mathbf{r}') \frac{dq(\mathbf{r}')}{dn} - q(\mathbf{r}') \frac{d}{dn} G(\mathbf{r} \mid \mathbf{r}') \right] dS \tag{2}$$

where $q(\mathbf{r})$ is the complex sound pressure inside the region with surface S and,

$$G(\mathbf{r} \mid \mathbf{r}') = \frac{e^{-ik|\mathbf{r}-\mathbf{r}'|}}{4\pi|\mathbf{r}-\mathbf{r}'|} \tag{3}$$

is the free space Greens function (the idealised sound pressure produced by a point source) for a sound source radiating sound at positive radian frequency ω and with wave number $k = \omega c$ where c is the speed of sound.

A remarkable feature of this integral equation is that the sound pressure outside the region is zero. This is possible because the sound pressure inside the region is produced by a combination of monopoles (the Greens function) and normally oriented dipoles (the normal gradient of the Greens function) which allows sound to be directed into the region and sound radiating out of the region to be cancelled [14].

For the case of an acoustic half-space divided by a plane the K–H integral simplifies and the sound field on one side of the plane may be described in terms of the pressure or the pressure velocity produced on the surface by sound sources in the other half-space. In effect, there is no need to cancel sound radiating out of the region because it is of infinite extent.

The two cor-responding integral formulas are known as Rayleigh's first and second integral formulas [13]. We consider the first integral formula here for $z > z_0$.

This equation states that the sound field for $z > z_0$ is the integral over the (x',y') plane positioned at $z = z_0$ of the sound pressure produced by a distribution of monopoles with amplitudes given by the normal component of the complex sound velocity in the (x',y') plane produced by sound sources in the half space $z < z_0$.

$$q(x,y,z) = \frac{-i\rho ck}{2\pi} \int_{-\infty}^{\infty} \int_{-\infty}^{\infty} v_z(x',y',z_0) \frac{e^{-ik|\mathbf{r}-\mathbf{r}'|}}{|\mathbf{r}-\mathbf{r}'|} dx'dy' \tag{4}$$

In other words, if we know the sound field on a plane and there are no sound sources in front of it, we can calculate the field at all points in front of the plane, because the sound propagates according to the wave equation.

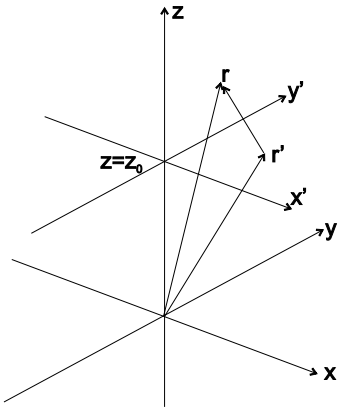

Figure 2: Rayleigh integral.

To simplify our description, we will now consider the 2D case where the sound field is constant in y. This would occur if the sound field was a combination of plane waves which were constant in y, or for a combination of line sources aligned parallel to the y axis. The Rayleigh integral can be simplified because the velocity is no longer a function of y and the integral of the 3D Greens function over y is known. For a point source at (x',y',z') the integral of the Greens function over y' is:

$$\int_{-\infty}^{\infty} \frac{e^{-ik|\mathbf{r}-\mathbf{r}'|}}{4\pi|\mathbf{r}-\mathbf{r}'|} dy' = \frac{i}{4} H_0^{(2)}(kR) \tag{5}$$

where $H_0^{(2)}(kR)$ is the cylindrical Bessel function of the second kind and $R = \mathrm{sqrt}[(x-x')^2+(z-z')^2]$ is the polar radius in the (x,z) plane.

The Rayleigh integral becomes [13]:

$$q(x,z) = \frac{\rho ck}{2} \times$$

$$\int_{-\infty}^{\infty} v_z(x',z_0) H_0^{(2)}\left(k\sqrt{(x-x')^2+(z-z_0)^2}\right) dx' \tag{6}$$

for $z > z_0$. This equation states that the 2D complex pressure can be reproduced for $z > z_0$ by a continuous distribution of line sources at $z = z_0$, each with complex amplitude .

For example, a line source at produces the complex pressure

$$q_S(x,z) = H_0^{(2)}\left(k\sqrt{x^2+(z-z_s)^2}\right) \tag{7}$$

The z-component of the velocity at $z = 0$ is

$$v_z(x,z) = \frac{i}{\rho\omega}\frac{dq_S(x,z)}{dz}\Big|_{z=0}$$
$$= \frac{i}{\rho c}H_0'^{(2)}\left(k\sqrt{x^2+z_s^2}\right)\frac{-z_s}{\sqrt{x^2+z_s^2}} \quad (8)$$

A Matlab simulation was written to demonstrate reproduction of a line source field, using a finite array of 250 sources over -20 to 20 metres (sources are 160 mm apart). The amplitudes of the 25 sources at each end of the array were tapered to zero using a raised cosine window to reduce end-effects [3], [6], [15].

The sound pressure produced by the line source is shown in Fig. 3 and the real and imaginary parts of the sound pressure reproduced by the line source array, calculated over –2 to 2 m, in x and z, are shown in Figs. 4 and 5. The line sources are shown as circles at $z = 0$. The WFS array reproduces the sound field correctly for $z > 0$, and produces the same sound field for $z < 0$, since the line sources radiate equally in both directions.

The reproduction error, defined as

$$e(x,z) = \frac{|q(x,z) - q_S(x,z)|}{|q_S(0,0)|} \quad (9)$$

is shown in Fig. 6. The error is below –40 dB in the reproduction half-space, except for positions close to the line sources. For $z <$ 0 the error is large since the WFS array generates a symmetric field, and is not able to generate a sound field that propagates towards it from the line source.

TIME REVERSAL – FOCUSED SOURCES

Time reversal is a technique that allows imaging of sound sources in homogenous media [7][8]. The sound pressure produced by one or more sources in the medium is detected at a number of points on a surface by an array of sensors. If the recorded signals are played back into the sensors (which can operate in reverse), the sound field will consist of wave fronts converging from the sensor array to the original sound source locations [8].

Time reversal can be implemented using the Rayleigh integral approach discussed in the previous section. The time-dependent complex pressure has the form, for $z > z_0$ (Eq (6))

$$q(x,z,t) = \frac{\rho ck}{2}\times$$
$$\int_{-\infty}^{\infty} v_z(x',z_0)\,e^{i\omega t}H_0^{(2)}\left(k\sqrt{(x-x')^2+(z-z_0)^2}\right)dx' \quad (10)$$

If the time index is reversed, $t \rightarrow -t$ then $\exp(i\omega(-t)) = \exp(-i\omega t)$ and the integral becomes

$$q_{TR}(x,z,t) = \frac{\rho ck}{2}\times$$
$$\int_{-\infty}^{\infty} v_z(x',z_0)\,e^{-i\omega t}H_0^{(1)}\left(k\sqrt{(x-x')^2+(z-z_0)^2}\right)dx' \quad (11)$$

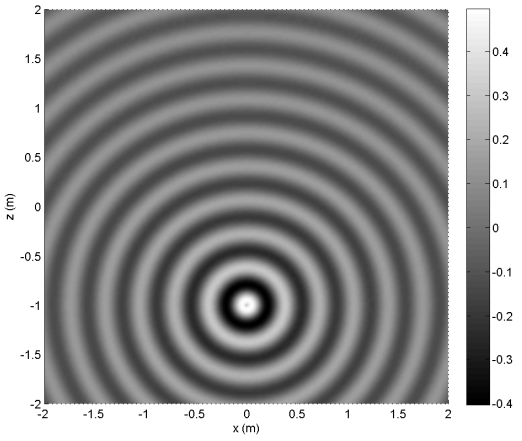

Figure 3: Line source sound field.

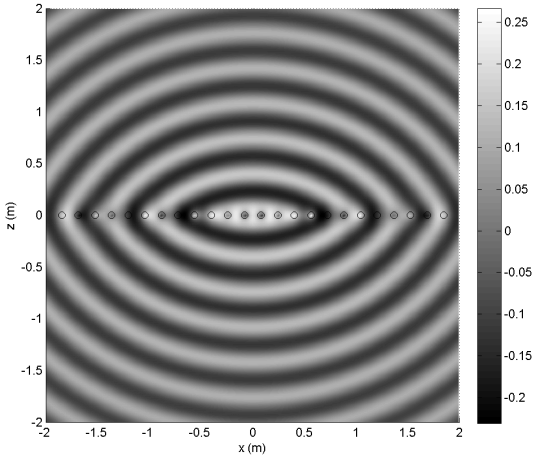

Figure 4: Real part of complex WFS field.

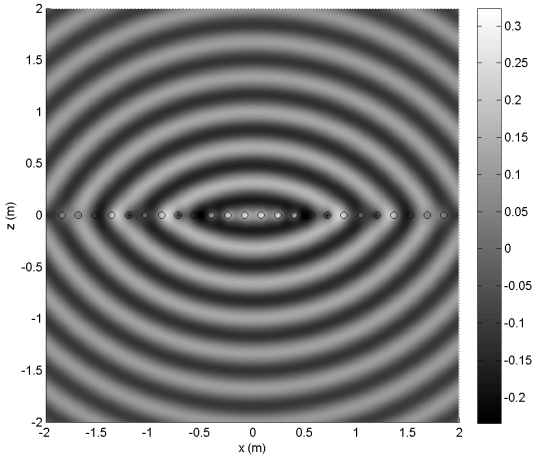

Figure 5: Imaginary part of complex WFS field.

where the Hankel function of the first kind (the conjugate of $H_0^{(2)}(kR)$) is required to produce wave propagation outward from each line source. The sound field produced by approximating this integral using the same discrete array as in Fig. 3 to Fig. 6 is shown in Fig. 7 and Fig. 8. The line array now produces circular wave fronts that converge on the source position as indicated by the arrows in Fig. 7. The same real sound pressure can be produced by conjugating the velocity, which is a well-known result in WFS theory.

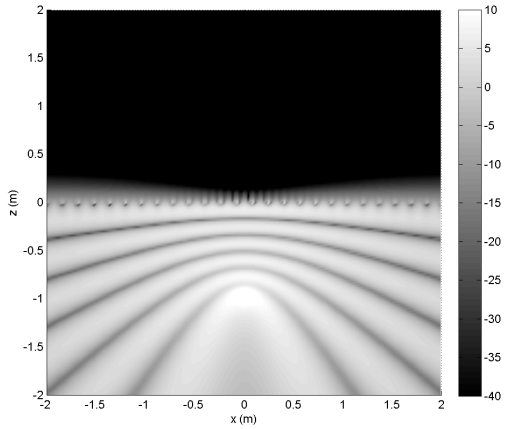

Figure 6: Error in dB.

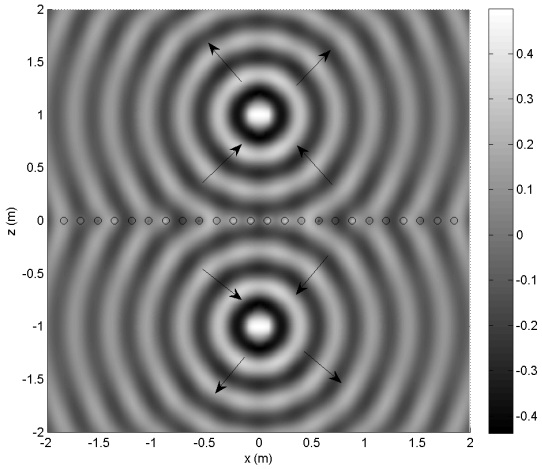

Figure 7: Real part of time-reversed sound field.

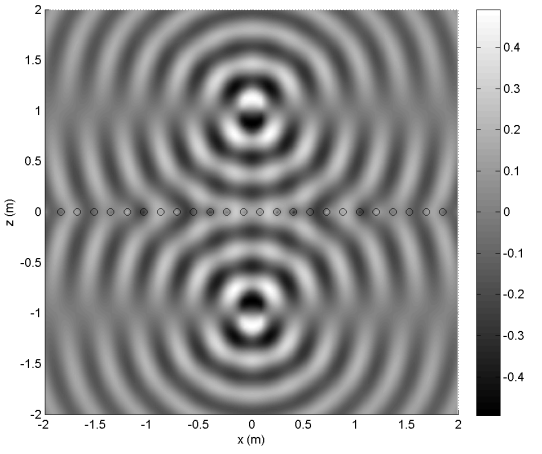

Figure 8: Imaginary part of time-reversed field.

The quadrature (imaginary) part of the field demonstrates circular wavefronts around each focus point with maxima on one side which align with the minima of the wavefronts on the other side, creating a discontinuity along a line between the two where the amplitude is zero. Since the observed sound field is given by Eq. (1), the quadrature field will be maximum at times $t_n = (n+1/2)/2f$ for integers n.

THEORETICAL DESCRIPTION OF A FOCUSED SOURCE

The sound reproduction example in the previous section generates two sets of focused sources, on each side of the array. One could ask the question, is it possible to generate a single focused source at the origin and is there a physical description of such a sound field?

Methods for generating such a field have been given in [10]–[12], [16]. A focused source may be described in two dimensions as a sum of plane waves arriving from angles from 0 to 180 degrees. Mathematically the focused source has the form

$$q_f(x,y) = \frac{1}{\pi}\int_0^{\pi} e^{i[kx\cos\phi_i + ky\sin\phi_i]}d\phi_i \tag{12}$$

where Φ is the azimuthal angle measured from the x-axis. This integral can be evaluated by expressing the plane wave in its cylindrical form using a Bessel expansion [13]

$$\begin{aligned} e^{ik(x\cos\phi_i + y\sin\phi_i)} &= e^{ikR\cos(\phi-\phi_i)} \\ &= \sum_{m=-\infty}^{\infty} i^m J_m(kR)\, e^{im(\phi-\phi_i)} \end{aligned} \tag{13}$$

For calculating the field over a finite radius R at wave number k, this expansion may be truncated to $m \in [-M,M]$ for $M=[kR]$ [17]. The integral can be carried out and the resulting expansion put in the form

$$q_f(R,\phi) = \sum_{m=-M}^{M} J_m(kR)\, e^{im\phi}\,\frac{\sin(m\pi/2)}{m\pi/2} \tag{14}$$

where the "sinc" function has the value of 1 for $m = 0$. The sound pressure at $R = 0$ is one since only the $m = 0$ term is nonzero for $R = 0$ and $J_0(0) = 1$. This sound field can be rotated by any angle Φ by using $(\Phi - \Phi_0)$ in the expansion.

The imaginary part of the sound field generated by this expansion is shown in Fig. 9, for a frequency of 1 kHz and Φ =-90 degrees. The sound field is similar to the focused source generated in each half space in Fig. 8. However, one can see interference effects which are caused by the plane waves arriving from 0 and 180 degrees, which create a standing wave component.

This effect can be reduced by limiting the range of integration from α to $\pi - \alpha$ for a small angle α. The sound field expansion becomes

$$q_{f,\alpha}(R,\phi) = \sum_{m=-M}^{M} J_m(kR)\, e^{im\phi}\,\frac{\sin(m(\pi/2-\alpha))}{m(\pi/2-\alpha)} \tag{15}$$

The wave field produced by this expansion for an angle α = 5 degrees is shown in Fig. 10. The standing wave interference is reduced from that appearing in Fig. 9 but is still noticeable.

A more general approach to generating a focused source is to allow the amplitudes of the plane waves to be weighted arbitrarily, instead of the equal weighting that occurs in Eq.s 14 and 15.

Continued on Page 18...

...Continued from Page 15.

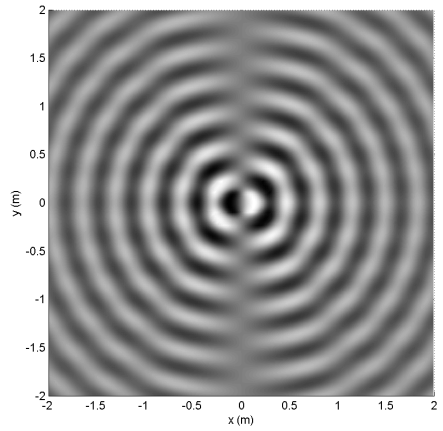

Figure 9: Quadrature focused source field using plane waves from 0 to 180 degrees.

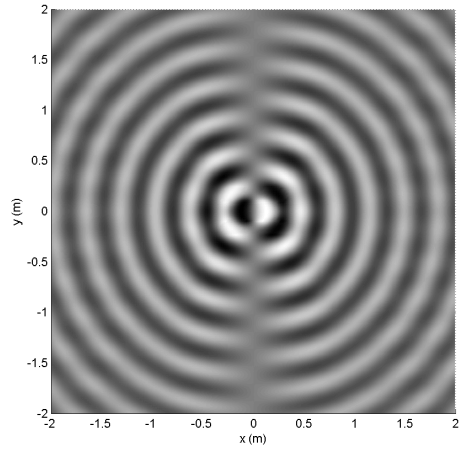

Figure 10: Quadrature focused source field using plane waves from 5 to 175 degrees.

We consider a focused source field given by,

$$q_{f,w}(x,y) = \frac{1}{2\pi}\int_0^{2\pi} e^{ikR\cos(\phi-\phi_i)} w(\phi_i)\, d\phi_i \tag{16}$$

where $w(\Phi_i)$ is a general window which will restrict the angles of arrival to between 0 and 180, of the form

$$w(\phi_i) = \sum_{m=-M}^{M} \beta_m e^{im\phi_i} \tag{17}$$

where the order of the window is limited to M, since this is the maximum order of the sound field expansion. Note that the order of the window may be less than M if desired by allowing some elements to be zero. Substituting this expansion and Eq. (13) into (16) yields

$$q_{f,w}(R,\phi) = \sum_{m=-M}^{M} i^m \beta_m J_m(kR) e^{im\phi} \tag{18}$$

A simple way to determine the coefficients β_m is to assume a rectangular window as above, determine the corresponding coefficients, and then apply a further windowing function to the coefficients to smooth the window. For a rectangular window of range α to $\pi - \alpha$ the coefficients are

$$\beta_m = \begin{cases} (-i)^m \dfrac{\sin\left[m(\pi/2-\alpha)\right]}{m(\pi/2-\alpha)}, & m \neq 0 \\ 1, & m = 0 \end{cases} \tag{19}$$

The effect of truncating the window order is to produce ringing in the window amplitude. A second window may be applied to the coefficients to reduce the effect. For example, the window produced for α = 10 degrees and M = 53 is shown in Fig. 11a, and the window produced by applying a Kaiser window to the coefficients is shown in 11b. The smoothed window rolls of the amplitude of the plane wave near 0 and 180 degrees and reduces ringing.

The sound field produced using 11b is shown in Fig. 12. The sound field shows less interference effects than those in Figs 9 and 10.

THE 3D CASE

The examples given above have all been for the 2D case where the sound pressure is a function of 2 coordinates only. The sources used in the WFS examples are line sources and the focused sources produced are line focused sources. Since we live in a 3D world, we will include a brief derivation of a focused source for the 3D case.

Following the previous section, we will generate a focused source from a distribution of plane waves arriving from angles (Θ_i, Φ_i) in spherical coordinates (Fig 13), (r, Θ, Φ)

$$q_{f,\alpha,3D}(x,y,z) = \frac{1}{2\pi}\int_0^{\pi/2-\alpha}\int_0^{2\pi} e^{ikr\left[\sin\theta\sin\theta_i\cos(\phi-\phi_i)+\cos\theta\cos\phi_i\right]} \sin\theta_i\, d\theta_i\, d\phi_i \tag{20}$$

where the plane waves are restricted to the upper hemisphere $\Theta_i \in [0, \pi/2 - \alpha]$ and where, as before, $\alpha > 0$ avoids plane waves arriving from $\Theta_i = \pi/2$ as these will produce standing waves. In the 3D case the standing wave is caused by plane waves arrive

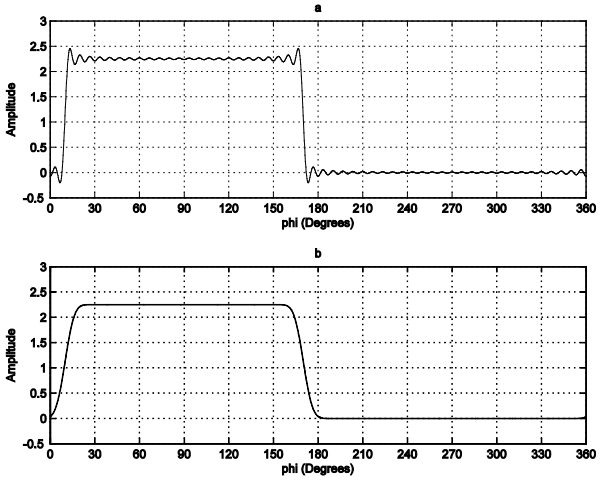

Figure 11: (a): Window for α = 10 degrees and (b) modified by a Kaiser window with Kaiser parameter 20.

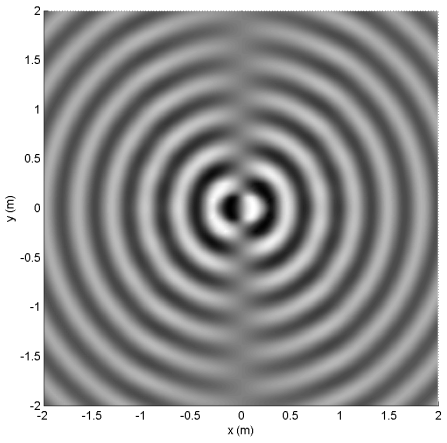

Figure 12: Quadrature focused source field using plane waves from 10 to 170 degrees with window smoothed by Kaiser window with Kaiser parameter 20

from all angles $\Phi_i \in [0, 2\pi]$.

Using the expansion in Eq. (13), it has the form

$$\int_0^{2\pi} e^{ikR\cos(\phi-\phi_i)}d\phi_i = J_0(kR) \tag{21}$$

which is a radial standing wave field.

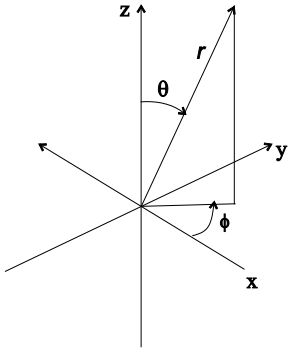

Figure 13: Spherical coordinates.

The integral in Eq. (20) can be carried out using the spherical harmonic expansion of the plane wave [13]

$$e^{ikr[\sin\theta\sin\theta_i\cos(\phi-\phi_i)+\cos\theta\cos\theta_i]} = 4\pi\sum_{n=0}^{\infty}\sum_{m=-n}^{n} i^n j_n(kr) Y_n^m(\theta,\phi) Y_n^m(\theta_i,\phi_i)^* \tag{22}$$

where $j_n(.)$ is the spherical Bessel function and

$$Y_n^m(\theta,\phi) = \sqrt{\frac{2n+1}{4\pi}\frac{(n-|m|)!}{(n+|m|)!}} P_n^{|m|}(\cos\theta) e^{im\phi} \tag{23}$$

is the $(n,m)th$ spherical harmonic, where $P_n^m(.)$ is the associated Legendre function.

Substituting Eq. (22) into (20) yields

$$q_{f,\alpha,3D}(r,\theta,\phi) = 2\sum_{n=0}^{\infty}\sum_{m=-n}^{n} i^n j_n(kr) Y_n^m(\theta,\phi)\times \int_0^{\pi/2-\alpha}\int_0^{2\pi} Y_n^m(\theta_i,\phi_i)^* \sin\theta_i d\theta_i d\phi_i \tag{24}$$

The integral over Φ_i eliminates all terms except the $m = 0$ term and produces a field which is rotationally symmetric

$$q_{f,\alpha,3D}(r,\theta) = \sum_{n=0}^{\infty} i^n j_n(kr)(2n+1) P_n(\cos\theta)\times \int_0^{\pi/2-\alpha} P_n(\cos\theta_i)\sin\theta_i d\theta_i \tag{25}$$

For the $n = 0$ case $P_0(\cos\Theta_i) = 1$ and the integral may be carried out directly yielding

$$\int_0^{\pi/2-\alpha} \sin\theta_i d\theta_i = 1-\cos(\pi/2-\alpha) \tag{26}$$

For $n > 0$ the integral may be carried out by substituting $u = \cos\Theta_i$ and using the recurrence formula [13]

$$(2n+1)P_n(u) = \frac{dP_{n+1}(u)}{du} - \frac{dP_{n-1}(u)}{du} \tag{27}$$

yielding

$$\int_{\cos\gamma}^{1} P_n(u)\,du = \frac{1}{2n+1}\left[P_{n-1}(\cos\gamma) - P_{n+1}(\cos\gamma)\right] \tag{28}$$

the final result is Eqn (29):

$$q_{f,\alpha,3D}(r,\theta) = j_0(kr)\left[1-\cos\left(\frac{\pi}{2}-\alpha\right)\right] + \sum_{n=1}^{\infty} i^n j_n(kr)(2n+1)P_n(\cos\theta)\times \left[P_{n-1}\left[\cos\left(\frac{\pi}{2}-\alpha\right)\right] - P_{n+1}\left[\cos\left(\frac{\pi}{2}-\alpha\right)\right]\right] \tag{29}$$

The field generated by this equation for a frequency of 1 kHz and $\alpha = 5$ degrees is shown in Fig. 14. The field looks similar to that of the 2D case in Fig. (12). However, in the 3D case the sound pressure will reduce with $1/r$ as opposed to 1/sqrt(R) in the 2D case.

As in the 2D case, the sound field shows some artefacts due to the interference of waves arriving over all azimuthal angles, in a similar manner to the 2D case. These artefacts could be reduced by applying a window $w(\Theta_i)$ to the plane wave integral in Eq. (20).

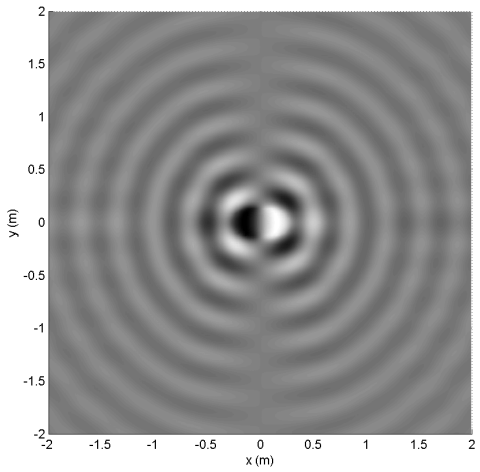

Figure 14: Quadrature focused source field in 3D using plane waves arriving from 0 to 85 degrees in elevation and 0 to 360 in azimuth.

Since the Legendre functions are orthogonal,

$$\int_0^{\pi} P_n(\cos\theta_i) P_m(\cos\theta_i) \sin\theta_i d\theta_i = \begin{cases} \dfrac{2}{2n+1}, n = m \\ 0, \quad n \neq m \end{cases} \tag{30}$$

this window can be written

$$w(\theta_i) = \sum_{n=0}^{M} \beta_n P_n(\cos\theta_i) \tag{31}$$

and the coefficients β_n may be obtained as

$$\beta_n = \frac{2n+1}{2} \int_0^{\pi} w(\theta_i) P_n(\cos\theta_i) \sin\theta_i d\theta_i \tag{32}$$

For a rectangular window

$$w(\theta_i) = \begin{cases} 1, \theta_i < \pi/2 - \alpha \\ 0, \theta_i > \pi/2 - \alpha \end{cases} \tag{33}$$

the coefficients can be calculated using the results above.

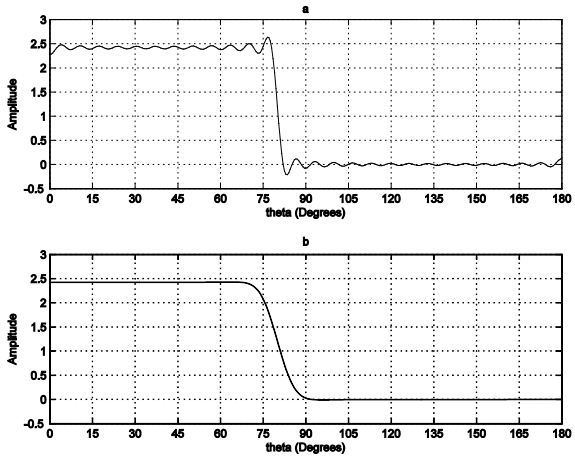

Figure 15a: Rectangular window for α = 10 degrees and M = 53. 15b: Window with additional Gaussian smoothing with γ = 10.

For a normalized sound pressure of one at the origin, the coefficients become

$$\beta_n = \frac{\left[P_{n-1}\left(\cos\left(\frac{\pi}{2} - \alpha\right)\right) - P_{n+1}\left(\cos\left(\frac{\pi}{2} - \alpha\right)\right)\right]}{1 - \cos\left(\frac{\pi}{2} - \alpha\right)} \tag{34}$$

for n > 0 and and β_0 = 1.

These coefficients can be weighted by a further window to reduce the effects of truncation and produce a tapering off of the plane wave amplitudes near $\Theta_i = \pi / 2 - \alpha$. Since the expansion in Eq. (31) is for positive integers n, the window must be one-sided to leave the low order terms unaltered. We will use a Gaussian window of the form

$$G(n) = e^{-\gamma(n/M)^2}, n \in [0, M] \tag{35}$$

with a window parameter γ that controls the rolloff. The window generated for α = 10 degrees and M = 53 is shown in Fig. 15a and the window produced by the Gaussian smoothing for γ = 10 is shown in Fig. 15b.

The resulting sound field is shown in Fig. 16. The wavefronts show less artefacts than Fig. 14.

CONCLUSION

This article has discussed the occurrence of focused sources which can arise naturally in reflections from curved surfaces at high frequencies and in sound re-production with time reversal. It has also been shown that focused source fields can be directly generated using a simple model based on plane waves arriving over a half space. Bessel expansions have been derived for both the 2D and 3D case and a windowing method presented for reducing artifacts in the repro-duced field. The imaginary part of the complex sound field shows wavefronts in the two half-spaces with a discontinuity along a line separating the half-spaces. The sound field is similar to the logo of the Acoustical Society of New Zealand, demonstrating that the logo has a physical basis.

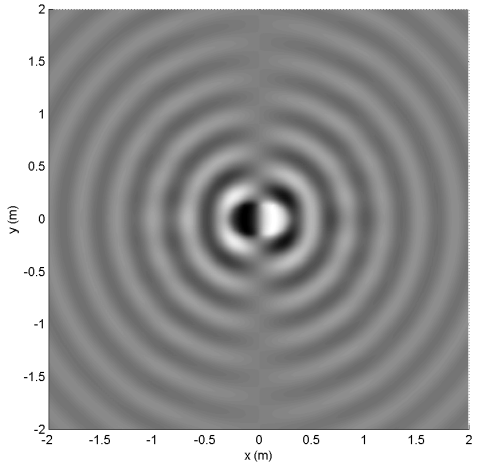

Figure 16: Quadrature focused source field in 3D using plane waves arriving from 0 to 80 degrees with Gaussian smoothing, γ = 10.

REFERENCES

[1] L. Cremer, H. A. Muller, and T. J. Schultz, Principles and applications of room acoustics. London: Applied Science Publishers, 1978.

[2] R. W. B. Stephens and A. E. Bate, Acoustics and Vibrational Physics, Second. London: Edward Arnold Ltd, 1966.

[3] E. N. G. Verheijen, "Sound reproduction by wave field synthesis," Delft university of technology, 1997.

[4] A. J. Berkhout, D. de Vries, and P. Vogel, "Acoustic control by wave field synthesis," J. Acoust. Soc. Am., vol. 93, no. 5, pp. 2764–2778, 1993.

[5] A. J. Berkhout, D. de Vries, and J. J. Sonke, "Array technology for acoustic wave field synthesis in enclosures," J. Acoust. Soc. Am., vol. 102, no. 5, pp. 2757–2770, 1997.

[6] S. Spors, R. Rabenstein, and J. Ahrens, "The Theory of Wave Field Synthesis Revisited," in AES 124th Convention, 2008, vol. 124.

[7] M. Fink, "Time reversal of ultrasonic fields - Part I: Basic principles," IEEE Trans. Ultrason. Ferroelectr. Freq. Control, vol. 39, no. 5, pp. 555–566, 1992.

[8] S. Yon, M. Tanter, and M. Fink, "Sound focusing in rooms: the time-reversal approach.," J. Acoust. Soc. Am., vol. 113, no. 3, pp. 1533–1543, 2003.

[9] S. Yon, M. Tanter, and M. Fink, "Sound focusing in rooms. II. The spatio-temporal inverse filter.," J. Acoust. Soc. Am., vol. 114, no. 6 Pt 1, pp. 3044–3052, 2003.

[10] J. Ahrens and S. Spors, "Focusing of Virtual Sound Sources in Higher Order Ambisonics," in AES 124th Convention, 2008.

[11] S. Spors, H. Wierstorf, M. Geier, and J. Ahrens, "Physical and Perceptual Properties of Focused Sources in Wave Field Synthesis," in AES 127th Convention, 2009.

[12] M. A. Poletti, "Improved methods for generating focused sources using circular arrays," in AES 133rd convention, 2012.

[13] E. G. Williams, Fourier Acoustics. San Deigo: Academic Press, 1999.

[14] M. A. Poletti, F. M. Fazi, and P. A. Nelson, "Sound-field reproduction systems using variable-directivity loudspeakers," J. Acoust. Soc. Am., vol. 129, no. 2, pp. 1429–1438, 2011.

[15] M. M. Boone, E. N. G. Verheijen, and P. F. Van Tol, "Spatial sound-field reproduction by wave-field synthesis," J. Audio Eng. Soc., vol. 43, no. 12, pp. 1003–1012, 1995.

[16] J. Ahrens and S. Spors, "Spatial encoding and decoding of focused virtual sound sources," in Ambisonics Symposium, 2009.

[17] D. B. Ward and T. D. Abhayapala, "Reproduction of a plane-wave sound field using an array of loudspeakers," IEEE Trans. Speech Audio Process., vol. 9, 6, pp. 697 – 707, 2001. ¶